# Acoustic-wave nonlinearity in stimulated Brillouin scattering

**Bruce S. Masson**

*Phillips Laboratory, Kirtland Air Force Base, New Mexico 87117-5776*

**Evangelos A. Coutsias**

*Department of Mathematics and Statistics, University of New Mexico, Albuquerque, New Mexico 87131*

Received April 27, 1993; revised manuscript received March 4, 1994

Stimulated Brillouin scattering is investigated here under conditions characterized by high optical pump intensity. Calculations are carried out at 1.3 and 3.8 $\mu$m with pump intensities equal to approximately three times the threshold. Such strong optical forcing leads to significant self-distortion of the density profile in the material wave serving as the optical grating. The method of multiple scales is used to find a uniform asymptotic expansion in the coupling. At the first perturbation level the resonant portion of the problem yields abridged equations for the incident and the scattered waves with frequencies $\omega_L$ and $\omega_S = \omega_L - \Omega$ and for the grating and its harmonics with frequencies $n\Omega$. The nonresonant portion of the first perturbation yields field components with the frequencies $\omega_L + n\Omega$ and $\omega_S - n\Omega$ for $n = 1, 2, \ldots$. Numerical solutions of the truncated abridged system are found by a method of Chebychev collocation and indicate a reduction in the observed phonon lifetime and a broadening of the linewidth with increasing amplitude.

## 1. INTRODUCTION

From the original nonlinear resonance ideas put forth by Bloembergen[1,2] to the discovery of the Riemann solution to the linear problem by Wang,[3] and through the numerical algorithms[4] available today, much of the understanding of stimulated scattering is based on the approximation that the scattering medium supports a linear response to the imposed forces. Accordingly the material wave is described by a simple sinusoid whose slowly varying complex amplitude represents a balance between the damping force, the driving force, and the transients. But in general a linear material response is an approximation that cannot be entirely accurate when the pump intensity exceeds the threshold intensity by some margin.

Although not specifically concerned with stimulated Brillouin scattering (SBS), one of the first investigations of electrostrictively forced nonlinear waves was carried out by Haus and Penfield.[5] More recently the effects of ion–acoustic wave nonlinearities were investigated[6] thoroughly and were found to alter the properties of SBS significantly in the plasmas generated during intense laser-beam-focusing experiments. In conventional fluids the acoustic speed is a function of the instantaneous temperature in gases or the instantaneous density in liquids, and hence the compressed regions or crests of the material wave overtake the rarefied regions or troughs of the wave. If this overtaking time becomes comparable with the phonon lifetime then the material wave assumes a distorted, nonsinusoidal profile.[7] Since the damping rate of the $n$th harmonic of the fundamental increases as $n^2$, the effective damping rate of the material wave increases as the amplitudes of the higher harmonics increase in magnitude. This leads to an apparent decrease in the observed phonon lifetime and a broadening of the linewidth.

To account for the nonlinear material-wave response, we employ the nonlinear wave equation for the velocity potential function first suggested by Kuznetsov[8] for problems in nonlinear acoustics. In addition to the nonlinearity that arises from the sound speed's dependence on the instantaneous thermodynamic state, Kuznetsov's equation also includes a comparably sized nonlinear contribution associated with an in-phase velocity gust that adds to the speed of the wave crests and subtracts from the speed of the wave troughs, thereby accelerating the overtaking process. The extension of Kuznetsov's equation to electrostrictive forcing was discussed previously.[7] Interestingly, the forced Kuznetsov equation does not alter in a fundamental way the underlying three-wave nonlinear resonance structure of the SBS problem. The rich multiple periodicity[9–11] of Floquet theory is still contained in the electromagnetic wave equation with its periodic but now nonsinusoidal coefficient. In Section 3 of this paper we employ multiple scaling to find the modified form of the abridged equations, including the case of a phase mismatch (an offset in the wave number or phase-matching condition).

In Section 4 we discuss the numerical solution of the truncated system of equations for the fundamental and its first three harmonics by a method of Chebychev collocation,[12] and in Section 5 we present numerical results for laser pulses of 1.315 and 3.8 $\mu$m scattered in xenon. Although there is noticeable amplitude in the higher harmonics in both cases the longer wavelength is, as might be expected from its longer phonon lifetime, more strongly affected.

0740-3224/94/081367-07$06.00 

## 2. NONDIMENSIONAL FORMULATION

Consider an otherwise quiescent fluid with sound speed $a_0$ and light speed $c_0$. Choose the SBS interaction zone to lie in the interval $0 < z < l$. To the left ($z < 0$) and to the right ($z > l$) the coupling should be thought of as being turned off, there being no grating and no scattering in either region. Let the incident wave be incoming (in the positive $z$ direction) with wave number $k_L$ and frequency $\omega_L$, the backscattered wave be outgoing (in the negative $z$ direction) with wave number $k_S$ and frequency $\omega_S$, and the grating modulation be traveling in the positive $z$ direction with wave number $q$ and frequency $\Omega$. To be specific, we assume that the frequency $\omega_L$ is specified and that $k_L$, $k_S$, and $\omega_S$ are calculated from the nondispersive relations of the undisturbed medium and the Doppler formula, that is,

$$\omega_L = c_0 k_L ,$$

$$\omega_S = c_0 k_S ,$$

$$\omega_L - \omega_S = a_0(k_L + k_S) .$$

The phase-matching condition determines $q$ when the mismatch parameter $q_1$ is specified,

$$q = (k_L + k_S)(1 - \epsilon q_1) .$$

Here $\epsilon$ is a small parameter (defined below) describing the amplitude of the grating, and $q_1$ is an order-unity parameter determining the degree of phase offset. The modulation frequency is then given by

$$\Omega = a_0 q .$$

For resonant behavior to occur, the phase offset must be restricted[13] to small excursions, $\epsilon q_1$, from the center value given by the Bragg condition, $q = k_L + k_S$.

We adopt the convention of denoting nondimensional variables by hats and subsequently dropping the hats when the nondimensionalization is complete. The nondimensional coordinates, $\hat{z}$, $\hat{t}$, and $\hat{\tau}$ are defined as

$$\hat{z} = qz ,$$

$$\hat{t} = (qa_0)t ,$$

$$\hat{\tau} = (qc_0)t .$$

It is seen that the spatial coordinate is defined such that the grating period is always $2\pi$ even when $q_1 \neq 0$, and the two time variables $\hat{t}$ and $\hat{\tau}$ apply to the grating and the optical fields, respectively.

The electric field is referenced to the square root of the incident peak value of the intensity, $I_L$, divided by the speed of propagation,

$$E = \sqrt{I_L/c_0\epsilon_0}\,\hat{E} ,$$

and the grating amplitude is characterized by the quantity $v_m$, representing the maximum material velocity induced in the grating, with the associated small-amplitude parameter $\epsilon$ defined as

$$\epsilon = v_m/a_0 \ll 1 .$$

The scalar electric field $\hat{E}(z, t)$ then satisfies the electromagnetic wave equation

$$E_{\tau\tau} - E_{zz} = -\epsilon g_1(\delta E)_{\tau\tau} , \tag{1}$$

where the hats have been dropped from the nondimensional variables. The $O(1)$ density variable $\delta$ is defined by

$$\epsilon\delta = (\rho - \rho_0)/\rho_0 ,$$

and the scattering strength $g_1$ as

$$g_1 = 2\rho_0 n_0'/n_0 ,$$

where $n_0' = \mathrm{d}n_0/\mathrm{d}\rho$. As is noted above, $\delta(z, t)$ has a spatial period of $2\pi$.

The grating modulation is described in terms of a velocity potential $\phi$ whose gradient is the material velocity. The nondimensionalization is chosen to be

$$\phi = (\epsilon a_0/q)\hat{\phi} ,$$

which yields an $O(1)$ value for the gradient of $\phi$ in the neighborhood of the maximum grating amplitude. The forced Kuznetsov equation[7] may then be written in terms of these nondimensional variables as

$$\phi_{tt} - \phi_{zz} = \epsilon\partial_t[(1/R)\phi_{zz} - (\gamma - 1)\phi_t\phi_t/2 - \phi_z\phi_z + g_2\langle E^2\rangle/2], \tag{2}$$

where $\langle E^2\rangle$ denotes the temporal average of $E^2$ taken over a time interval that is long compared with the optical period but short compared with the acoustic period. The remaining quantities are

$$(\gamma - 1)/2 = \mathrm{d}(\log a)/\mathrm{d}(\log \rho) ,$$

$$R = \epsilon a_0/\nu_0 q ,$$

$$g_2 = \chi_0' I_L/a_0^2 c_0 \epsilon^2 .$$

Here $\chi_0' = \mathrm{d}\chi_0/\mathrm{d}\rho$ and $\nu_0$ is the acoustic diffusivity,[8]

$$\nu_0 = (\lambda_0 + 2\mu_0)/\rho_0 + (\kappa_0/\rho_0 c_v)(c_p - c_v)/\rho_0 a_0^2 \kappa_T c_v ,$$

with $\lambda_0$ and $\mu_0$ denoting the bulk and the shear viscosities, $\kappa_0$ the thermal conductivity, and $\kappa_T$ the isothermal compressibility. The quantities $c_p$ and $c_v$ are the two specific heats of the fluid. The density is then found from[7]

$$\delta_t = -\phi_{zz} - \epsilon\partial_t(\phi_t\phi_t - \phi_z\phi_z) , \tag{3}$$

after we again drop the hats. From this point forward all variables are nondimensional and without hats. Physical parameters remain dimensional and without hats, but there should be no confusion between the two.

Digressing for a moment, consider Eqs. (1) and (2) individually. Equation (1) is the wave equation describing coherent optical scattering from a traveling-wave grating specified by the periodic coefficient $\delta(z, t)$. In linear problems this type of equation leads naturally to a Hill differential equation for the eigenfunctions. From Floquet theory it is known that these eigenfunctions are either multiply periodic (stable) oscillations or ex-

ponentially attenuated or growing (unstable) oscillations (excluding exceptional cases corresponding to zone boundaries). The stable eigenfunctions describe transmission, while unstable eigenfunctions describe reflection. In the nonresonant problem the field is described by an eigenfunction expansion [for sinusoidal gratings[9–11] these are the Mathieu functions $F_n^{(\nu)}(z)$, one from each stability interval $n = 1, 2, \ldots$ with the Floquet exponent $\nu$], and there will be multiple scattered waves at the frequencies $\omega_L \pm n\Omega$.

On the other hand, consider Eq. (2) on its own with $\langle E^2 \rangle$ thought of as a periodic, externally derived, driving force. The underlying structure of the solution is that of a weakly nonlinear wave experiencing viscous damping and resonant periodic forcing. After the initial transient dies out, the solution consists of a single traveling wave at the forcing period whose amplitude represents a balance between viscous damping, weak nonlinearity, and the driving force. The parameter $R$ apportions the balance between the linear (viscous) and the nonlinear loss mechanisms.

## 3. MULTIPLE SCALES

Because of the resonant nature of the three-wave interaction, a conventional perturbation series would be expected to fail through the appearance of algebraically unbounded (secular) terms growing in proportion to $t$ at some stage of the expansion, say at $E^{(n)}$ and $\phi^{(n)}$. In multiscaling, the asymptotic ordering of the series is regained when the definitions of $E^{(n)}$ and $\phi^{(n)}$ are extended to include functional dependencies on additional independent variables designed to capture slow changes and to avoid the necessity of expanding exponential functions of $\epsilon t$ by Taylor series. At the first order, multiscaling leads to the same results as the slowly varying envelope approximation, but multiscaling permits a broader view of the underlying structure.

The expansions in powers of $\epsilon$ are taken in the form

$$E = \sum_{n=0}^{\infty} \epsilon^n E^{(n)}(z, \tau; \tilde{z}, \tilde{\tau}, \tilde{t}), \tag{4}$$

$$\phi = \sum_{n=0}^{\infty} \epsilon^n \phi^{(n)}(z, t; \tilde{z}, \tilde{t}), \tag{5}$$

where the slow variables $\tilde{z}$, $\tilde{t}$, and $\tilde{\tau}$ are introduced to capture the secular changes directly,

$$\tilde{z} = \epsilon z,$$
$$\tilde{t} = \epsilon t,$$
$$\tilde{\tau} = \epsilon \tau.$$

Derivatives of $E^{(n)}(z, \tau; \tilde{z}, \tilde{\tau}, \tilde{t})$ and $\phi^{(n)}(z, t; \tilde{z}, \tilde{t})$ are calculated by the chain rule,

$$\partial_t = \partial_t + \epsilon \partial_{\tilde{t}},$$

and similarly for the other two variables $\tau$ and $z$. The differentiation indicated on the left-hand side is applied to $E^{(n)}(z, t)$ or $\phi^{(n)}(z, t)$, and the differentiations indicated on the right-hand side are applied to $E^{(n)}(z, \tau; \tilde{z}, \tilde{\tau}, \tilde{t})$ or $\phi^{(n)}(z, t; \tilde{z}, \tilde{t})$. Thus $\partial_t$ has a different meaning on the two sides of the equation, with different variables being held constant. After two applications of the chain rule, the wave operator on the left-hand side of Eq. (1) becomes

$$\partial_{\tau\tau} - \partial_{zz} = \partial_{\tau\tau} - \partial_{zz} + 2\epsilon(\partial_{\tau\tilde{\tau}} - \partial_{z\tilde{z}}) + O(\epsilon^2),$$

with a similar expression holding for the wave operator on the left-hand side of Eq. (2) with $t$ substituted everywhere for $\tau$.

After substitution of the series in Eqs. (4) and (5) into Eqs. (1)–(3) and collection of like powers of $\epsilon$, the $O(1)$ equations are found to be

$$(\partial_{\tau\tau} - \partial_{zz})E^{(0)} = 0, \tag{6}$$

$$(\partial_{tt} - \partial_{zz})\phi^{(0)} = 0, \tag{7}$$

$$\delta^{(0)} = -\phi_t^{(0)}. \tag{8}$$

Collecting $O(\epsilon)$ terms gives

$$(\partial_{\tau\tau} - \partial_{zz})E^{(1)} = -2(\partial_{\tau\tilde{\tau}} - \partial_{z\tilde{z}})E^{(0)} - g_1 \partial_{\tau\tau}[\delta^{(0)} E^{(0)}], \tag{9}$$

$$\begin{aligned}(\partial_{tt} - \partial_{zz})\phi^{(1)} = &-2(\partial_{t\tilde{t}} - \partial_{z\tilde{z}})\phi^{(0)} \\ &+ \partial_t\{(1/R)\phi_{zz}^{(0)} - (\gamma - 1)[\phi_t^{(0)}]^2/2 \\ &- [\phi_z^{(0)}]^2 + g_2\langle [E^{(0)}]^2 \rangle/2\}.\end{aligned} \tag{10}$$

The functional dependence of $E^{(0)}(z, \tau; \tilde{z}, \tilde{\tau}, \tilde{t})$ and $\phi^{(0)}(z, t; \tilde{z}, \tilde{t})$ on the fast variables is determined at the zeroth order, that is, by Eqs. (6) and (7). The dependence on the slow variables is determined by the requirement that Eqs. (9) and (10) produce no secular terms in $E^{(1)}$. Using complex traveling-wave solutions of Eqs. (6) and (7) to evaluate the right-hand sides of Eqs. (9) and (10) shows that every term on the right-hand sides of the equations generates at least one contribution in the form of a complex traveling wave satisfying the homogeneous part of Eqs. (9) and (10). The solutions for $E^{(1)}(z, \tau; \tilde{z}, \tilde{\tau}, \tilde{t})$ and $\phi^{(1)}(z, t; \tilde{z}, \tilde{t})$ would then, by necessity, contain contributions growing in proportion to $\tau$ and $t$, respectively, unless the offending terms on the right-hand sides of Eqs. (9) and (10) sum to zero. Collecting like terms and setting the sum to zero gives the conditions necessary to determine the slow-variable dependence in $E^{(0)}(z, \tau; \tilde{z}, \tilde{\tau}, \tilde{t})$ or $\phi^{(0)}(z, t; \tilde{z}, \tilde{t})$.

Letting $e_L$, $e_S$, and $\sigma_n$ denote undetermined coefficients that can depend on the slow variables, we write solutions to Eqs. (6) and (7) in the form

$$\delta^{(0)} = -\phi_t^{(0)} = \sum_{n=-\infty}^{\infty} \sigma_n(\tilde{z}, \tilde{t}) \exp(in\theta), \tag{11}$$

$$E^{(0)} = e_L(\tilde{z}, \tilde{\tau}, \tilde{t}) \exp(i\xi) + e_S(\tilde{z}, \tilde{\tau}, \tilde{t}) \exp(i\eta) + \text{c.c.}, \tag{12}$$

where

$$\xi = (k_L/q)(z - \tau),$$
$$\eta = (k_S/q)(-z - \tau),$$
$$\theta = z - t.$$

Note that

$$\xi - \eta - \theta = q_1 \epsilon \theta \equiv q_1 \tilde{\theta},$$

where $\tilde{\theta} = \epsilon\theta$ is another slow variable. Equation (11) represents a period-1 (modulo the electrostrictive force)

traveling wave of arbitrary profile, as was anticipated earlier. For the moment taking $q_1 = 0$, we may rewrite Eq. (12) as

$$E^{(0)} = \exp(-i\beta\tau)\{e_L \exp[i(k_L/q)\theta] + e_S \exp[-i(k_S/q)\theta]\} + \text{c.c.},$$

where $\beta = 2k_Lk_S/q^2 \approx 1/2$. The factor $\exp(-i\beta\tau)$ is the Doppler-shifted harmonic time factor, and since $k_L/q \approx k_S/q \approx 1/2$, the factor in braces is just the period-2 spatial oscillation expected in the first Floquet unstable zone. The amplitude modulation corresponding to the real part of the Floquet exponent is contained in the amplitude factors $e_L$ and $e_S$.

The term $[E^{(0)}]^2$ in Eq. (10) generates two terms that also satisfy the homogeneous form of the equation and result in secular growth in $\phi^{(1)}$. The two are easily identified, since they may be written in terms of $\theta$ plus slow variables. Since $\theta = \xi - \eta + O(\epsilon)$, we have

$$[E^{(0)}]^2 = 2e_Le_S^* \exp[i(\xi - \eta)] + \text{c.c.} + \ldots, \quad (13)$$

where the dots indicate terms that do not produce secular behavior in $E^{(1)}$. Next consider the product $\delta^{(0)}E^{(0)}$ appearing in Eq. (9). The infinite series contributes four terms that produce secular behavior in $E^{(1)}$. The four are easily identified as those that can be written in terms of $\xi$ plus slow variables or $\eta$ plus slow variables. Since $\xi = \eta + \theta + O(\epsilon)$ etc., these terms can arise only when $n = 1$. We find then that

$$\delta^{(0)}E^{(0)} = \sigma_1^* e_L \exp[i(\xi - \theta)] + \sigma_1 e_S \exp[i(\eta + \theta)] + \text{c.c.} + \ldots, \quad (14)$$

where the dots again indicate terms that avoid secular behavior in $E^{(1)}$.

With the suppression of secular behavior it is possible to find the nonresonant contributions to $E^{(1)}$ and $\phi^{(1)}$ by solving Eqs. (9) and (10) for the forcing terms indicated by dots in Eqs. (13) and (14). The nonresonant parts of Eqs. (9) and (10) may be written as

$$(\partial_{\tau\tau} - \partial_{zz})E^{(1)} = -g_1\partial_{\tau\tau}\Bigg(\sum_{n=1}^{\infty}[e_L\sigma_n + e_S\sigma_{n+1}\exp(i\theta)] \times \exp\{i[(n+1)\xi - n\eta]\} + \sum_{n=1}^{\infty}[e_S\sigma_n^* + e_L\sigma_{n+1}^*\exp(-i\theta)] \times \exp\{i[(n+1)\eta - n\xi]\} + \text{c.c.}\Bigg),$$

$$(\partial_{tt} - \partial_{zz})\phi^{(1)} = 0.$$

Neglecting terms of $O(a_0/c_0)$, we find the solutions to be

$$E^{(1)} = (g_1/4)\Bigg\{\exp(i\xi)\sum_{n=1}^{\infty}[n^{-1}(n+1)^{-1}e_L\sigma_n + (n+1)^{-1}(n+2)^{-1}e_S\sigma_{n+1}\exp(i\theta)]\exp(in\theta) + \exp(i\eta)\sum_{n=1}^{\infty}[n^{-1}(n+1)^{-1}e_S\sigma_n^* + (n+1)^{-1}(n+2)^{-1}e_L\sigma_{n+1}^*\exp(-i\theta)] \times \exp(-in\theta) + \text{c.c.}\Bigg\},$$

$$\phi^{(1)} = 0.$$

It is seen that $E^{(1)}$ contains the frequencies $\omega_L + n\Omega$ and $\omega_S - n\Omega$ for $n = 1, 2\ldots$, in agreement with the results of Peng and Cassedy.[11]

The resonant part of Eq. (9) is found by setting the coefficients of $\exp(i\xi)$ and $\exp(i\eta)$ equal to zero and arriving at

$$(\partial_{\tilde{\tau}} + \partial_{\tilde{z}})e_L = (i/2)(g_1k_L/q)\sigma_1e_S\exp(-iq_1\tilde{\theta}), \quad (15)$$

$$(\partial_{\tilde{\tau}} - \partial_{\tilde{z}})e_S = (i/2)(g_1k_S/q)\sigma_1^*e_L\exp(iq_1\tilde{\theta}), \quad (16)$$

which are the usual abridged equations for the two optical waves. Similarly, the resonant part of Eq. (10) is found by setting each of the coefficients of $\exp(in\theta)$ equal to zero. Evaluating the individual terms in Eq. (10) in terms of $\sigma_n$ gives

$$\partial_{t\tilde{t}}\phi^{(0)} = -\sum_n \partial_{\tilde{t}}\sigma_n\exp(in\theta),$$

$$\partial_{z\tilde{z}}\phi^{(0)} = \sum_n \partial_{\tilde{z}}\sigma_n\exp(in\theta),$$

$$\partial_{zzt}\phi^{(0)} = \sum_n n^2\sigma_n\exp(in\theta),$$

$$\partial_t[(\gamma-1)[\phi_{\tilde{t}}^{(0)}]^2/2 + [\phi_{\tilde{z}}^{(0)}]^2] = i[(\gamma+1)/2]\sum_n n\Bigg(\sum_m \sigma_m\sigma_{n-m}\Bigg)\exp(in\theta).$$

The result for $n = 1$ is

$$(\partial_{\tilde{t}} + \partial_{\tilde{z}} + 1/2R)\sigma_1 - (i/4)(\gamma+1)\sum_{m=-\infty}^{\infty}\sigma_m\sigma_{1-m} = (i/2)g_2e_Le_S^*\exp(iq_1\tilde{\theta}), \quad (17)$$

and for $n > 1$ is

$$(\partial_{\tilde{t}} + \partial_{\tilde{z}} + n^2/2R)\sigma_n - (i/4)(\gamma+1)n\sum_{m=-\infty}^{\infty}\sigma_m\sigma_{n-m} = 0. \quad (18)$$

Since $\sigma_{-n} = \sigma_n^*$, these equations account for the complete behavior of $\delta^{(0)}$.

## 4. NUMERICAL SOLUTION

Our interest lies in conditions under which the incident pulse is long enough to permit the energy cascade to higher modes. That is, we assume that the pulse is slowly varying in time so that the time derivatives in Eqs. (15) and (16) are negligible. We also assume that the phase matching is exact, i.e., $q_1 = 0$, to maximize the coupling through the idler. The abridged equations are then separated into real and imaginary parts by the substitution

$$e_L = u_L\exp(i\phi_L),$$

$$e_S = u_S\exp(i\phi_S),$$

$$\sigma_n = \epsilon^{-1}u_n\exp(i\phi_n),$$

$n$ being a positive integer. The real parts of Eqs. (15)–(18) are found to be

$$\partial_\zeta u_L = -\alpha_L\Lambda u_1u_S\cos\Phi, \quad (19)$$

$$\partial_\zeta u_S = -\alpha_S\Lambda u_1u_L\cos\Phi, \quad (20)$$

$$(\partial_t + \Gamma)u_1 - 2A\sum_{m=1}^{\infty} u_{1+m}u_m \cos\Phi_{1m} = \alpha_1 u_L u_S \cos\Phi\,, \tag{21}$$

$$(\partial_t + n^2\Gamma)u_n - 2nA\sum_{m=1}^{\infty} u_{n+m}u_m \cos\Phi_{nm} + nA\sum_{m=1}^{n-1} u_{n-m}u_m \cos\Phi_{nm} = 0\,, \tag{22}$$

with

$$\zeta = 2\hat{z}/ql - 1\,,$$

where $l$ is the length of the interaction zone and $t$ is actually $\hat{t}$ with the hat omitted (as was done previously). The phase angles appearing here are

$$\Phi = \phi_1 + \phi_S - \phi_L - \pi/2\,,$$
$$\Phi_{nm} = \phi_{n+m} - \phi_m - \phi_n + \pi/2\,,$$
$$\Psi_{nm} = \phi_{n-m} + \phi_m - \phi_n - \pi/2\,,$$

and the nondimensional parameters are

$$\alpha_L = g_1 k_L/4q \approx \rho_0 n_0'/4n_0\,,$$
$$\alpha_S = g_1 k_S/4q \approx \alpha_L\,,$$
$$\alpha_1 = \epsilon^2 g_2/2 = \chi_0' I_L/2\alpha_0^2(c/n_0)\,,$$
$$\Gamma = \nu_0 q/2a_0\,,$$
$$\Lambda = ql\,,$$
$$A = (\gamma + 1)/4\,.$$

From the imaginary parts of Eqs. (15)–(18), we find

$$u_L\partial_\zeta\phi_L = -\alpha_L\Lambda u_1 u_S \sin\Phi\,,$$
$$u_S\partial_\zeta\phi_S = \alpha_S\Lambda u_1 u_L \sin\Phi\,,$$
$$u_1\partial_t\phi_1 - 2A\sum_{m=1}^{\infty} u_{1+m}u_m \sin\Phi_{1m} = -\alpha_1 u_L u_S \sin\Phi\,,$$
$$u_n\partial_t\phi_n - 2nA\sum_{m=1}^{\infty} u_{n+m}u_m \sin\Phi_{nm} + nA\sum_{m=1}^{n-1} u_{n-m}u_m \sin\Phi_{nm} = 0\,.$$

We assume that there is indeed a grating present, i.e., that the grating is organized and identifiable in the form of a slowly modulated periodic wave. In this case it is possible to identify a grating phase angle $\theta_0$ and to conclude that the individual phase angles, $\phi_n$, must have the form

$$\phi_n = \pi/2 - n\theta_0\,.$$

Substituting this expression into the definitions of $\Phi_{nm}$ and $\Psi_{nm}$, we find that

$$\Phi_{nm} = \Psi_{nm} = 0\,.$$

Then the equation for $\phi_1$ (the imaginary part of the equation for $\sigma_1$) demands that

$$\sin\Phi = 0\,.$$

Of the two choices $\Phi = 0$ and $\Phi = \pi$, the latter evolves quickly to the former by means of a phase jump as $u_1$ passes through zero. $\Phi = 0$ is the usual phase condition for maximum gain ($\theta_0 = \phi_S - \phi_L$).

Our numerical results will be for the system obtained by truncation of summations in Eqs. (21) and (22) after the fourth grating mode. In the numerical solutions the six real-valued unknowns consisting of the two field amplitudes and the four grating amplitudes are each represented by a 17-term expansion in spatially dependent Chebychev polynomials, $T_n(\zeta)$ [the definition of $\zeta$ follows Eq. (22)]. The coefficient multiplying each Chebychev polynomial is an undetermined function of time to be evaluated by means of spatial collocation of Eqs. (19)–(22). This yields a set of $4 \times 17$ ordinary differential equations in time for the same number of undetermined coefficients. The system of differential equations is marched forward in time, with an inversion of a full $34 \times 34$ matrix required at each function evaluation, to determine the optical amplitudes.

## 5. RESULTS

Results are presented in this section for optical pulses with wavelengths equal to 1.315 and 3.8 $\mu$m. The scattering cell contains 30-amagat xenon gas and is 30 cm long. The incident pulses are Gaussian in shape with an $e^{-1}$ amplitude width equal to 20 phonon lifetimes, i.e., $20/\nu_0 q^2$. Figure 1 shows an example of the temporal histories of $u_L{}^2$ and $u_S{}^2$ (intensities) for the 3.8-$\mu$m case with a peak incident intensity of $I_L = 70$ MW/cm$^2$. The horizontal axis in the figure is measured in units of the phonon lifetime, $t\nu_0 q^2$. The asymmetric compression of the scattered wave seen here is also observed for other conditions not near threshold. In these cases the scattered wave characteristically turns on late and follows the incident wave down to extinction. However, near threshold the compression becomes more symmetric, with the scattered wave preceding the incident wave to extinction. Defining the reflectivity in terms of the ratio of the scattered pulse energy to the incident pulse energy,

$$r = \int_{-\infty}^{\infty} u_S{}^2 \mathrm{d}t \Big/ \int_{-\infty}^{\infty} u_L{}^2 \mathrm{d}t\,,$$

provides a convenient definition of the threshold intensity, $I_{L,th}$, as that incident peak intensity for which the reflectivity extrapolates to zero. Such a reflectivity curve

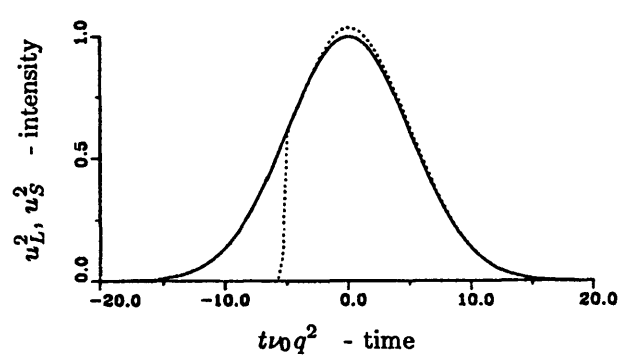


Fig. 1. Temporal variation of optical intensity. The solid curve is the incident 3.8-$\mu$m Gaussian pulse, $u_L{}^2$. The dotted curve is the computed scattered pulse, $u_S{}^2$, in xenon at 30 amagats. The relative time axis is scaled in units of the phonon lifetime, $1/\nu_0 q^2$, centered at the pulse peak. The peak intensity is 70 MW/cm$^2$.

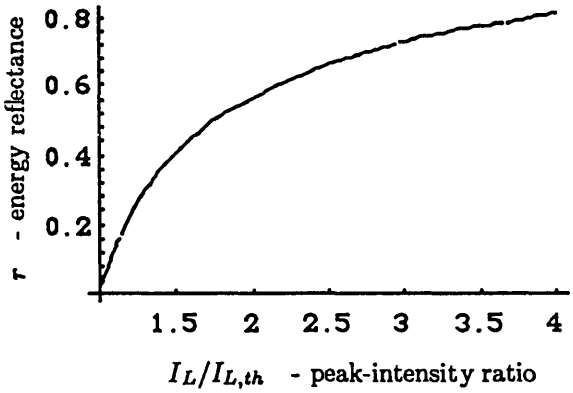


Fig. 2. Computed reflectivity for the backscattering of a 3.8-$\mu$m wavelength pulse in 30-amagat xenon gas as a function of the incident pulse peak intensity. $I_{L,\mathrm{th}}$ is the threshold pulse peak intensity, computed to be 20 MW/cm$^2$.

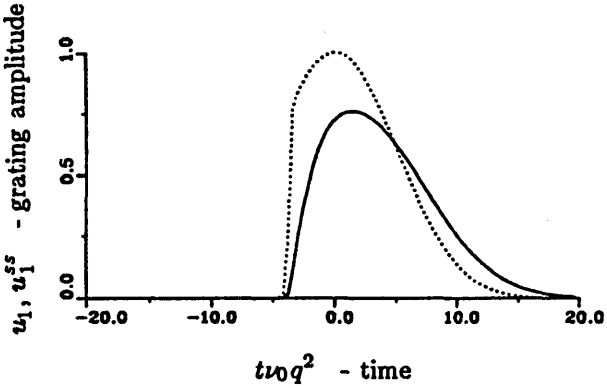


Fig. 3. Temporal variation of grating fundamental at the first node for a 3.8-$\mu$m pulse in 30-amagat xenon. The solid curve is the computed amplitude of the grating fundamental, $u_1$. The dotted curve is the quasi-steady amplitude $u_1{}^{ss}$. Both curves are normalized to the temporal peak of $u_1{}^{ss}$.

is shown in Fig. 2 plotted in terms of the ratio of incident peak values $I_L/I_{L,\mathrm{th}}$. For the cases presented here, $I_L/I_{L,\mathrm{th}} \approx 3$.

Figure 3 describes grating behavior found for the 3.8-$\mu$m pulse. The phonon lifetime $(\nu_0 q^2)^{-1} = 288$ ns is found by evaluation of the bulk viscosity $\lambda_0$, appearing in the expression for $\nu_0$ following Eq. (2) by use of the equality in the Stokes relation[14]

$$\lambda_0 + (2/3)\mu_0 \geq 0.$$

In Fig. 3 the temporal behavior of the fundamental grating amplitude $u_1$ at the first node is compared with the quasi-steady grating amplitude,

$$u_1{}^{ss} = \alpha_1 u_L u_S/\Gamma,$$

which we obtain by setting the time derivative in Eq. (21) equal to zero and neglecting the convolution sum. Both curves are normalized to the peak value of $u_1{}^{ss}$. Since $u_1$ peaks at nearly the same time as $u_1{}^{ss}$, the pulse lengths used here appear to be long enough to minimize the transient contribution, and the differences should be attributed to the nonlinearity of the grating and the cascade of acoustic energy into the higher modes. The depression of $u_1$ may be thought of as being equivalent to an increase in the effective diffusivity above its molecular value $\nu_0$. For comparison the results for 1.315 $\mu$m at a peak intensity of 110 MW/cm$^2$ are shown in Fig. 4. The phonon lifetime for this condition is computed to be 34.6 ns. The stronger damping experienced by the shorter-wavelength grating is evident from the shift of the grating peak amplitude to times later in the pulse than seen in Fig. 3.

The higher harmonics, $u_2/u_1$ (solid curves) and $u_3/u_2$ (dotted curves), are shown in Fig. 5. The upper pair of curves in the figure shows the grating amplitude ratios $u_2/u_1$ and $u_3/u_2$ for 3.8 $\mu$m, whereas the lower pair of curves refer to the 1.315-$\mu$m case. We believe that $u_3/u_2$ is probably influenced significantly by the brutal truncation that we employed (an improvement could be based on the results of Ref. 15). Figure 6 summarizes the results by showing the temporal peak values of $u_2/u_1$ found at various values of the reflectivity $r$ for the 3.8-$\mu$m case. The harmonic ratio $u_2/u_1$ is seen to grow linearly for small reflectivity.

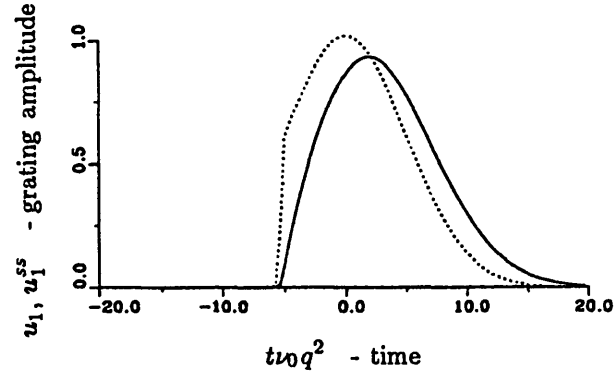


Fig. 4. Temporal variation of grating fundamental for a 1.315-$\mu$m pulse in 30-amagat xenon. The solid curve is the computed amplitude of the grating fundamental $u_1$. The dotted curve is the quasi-steady amplitude $u_1{}^{ss}$. Both curves are normalized to the temporal peak of $u_1{}^{ss}$.

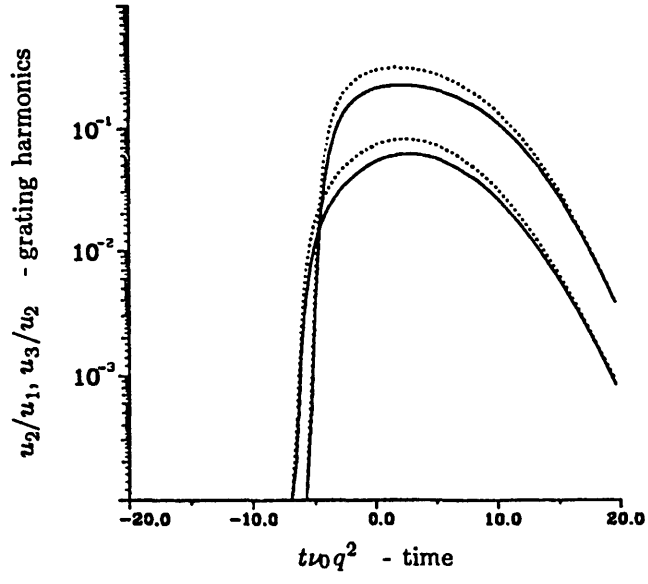


Fig. 5. Temporal variation of grating harmonic ratios for 3.8-$\mu$m (upper pair of curves) and 1.315-$\mu$m (lower pair) pulses. The solid curves are the amplitude ratios $u_2/u_1$. The dotted curves are the amplitude ratios $u_3/u_2$.

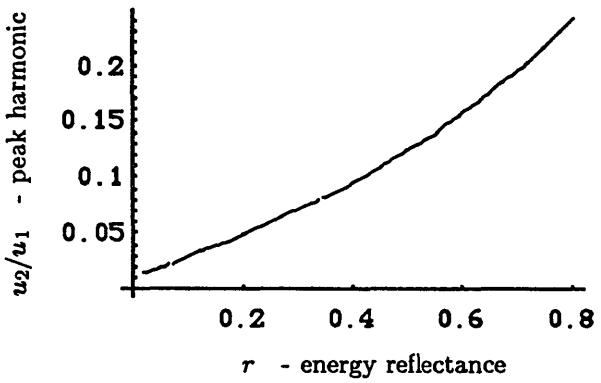


Fig. 6. Computed values of the maximum ratio $u_2/u_1$ versus the reflectivity $r$ for the 3.8-$\mu$m-wavelength pulse in 30 amagats of xenon.

## 6. CONCLUSIONS

The method of multiple scales was employed to investigate nonlinear acoustic response during stimulated Brillouin backscatter. The resonant problem led to a system of equations for the incident and the scattered fields with frequencies $\omega_L$ and $\omega_S$ and the grating at its fundamental $\Omega$ and its harmonics $n\Omega$. The nonresonant fields were also calculated in the first approximation, showing the presence of field components with frequencies $\omega_L + n\Omega$ and $\omega_S - n\Omega$ for $n = 1, 2, \ldots$. The one-dimensional model provides only an averaged view of the highly three-dimensional phenomena occurring during an actual SBS backreflection and will significantly underestimate the actual presence of grating harmonics. In general our conclusion drawn from the numerical study of the resonant problem is that the higher harmonics of the grating fundamental are always present to some degree but certainly more so at longer wavelengths. These higher harmonics lead to self-distortion of the SBS grating that can be significant in the infrared, where the phonon lifetimes can exceed 100 ns. At this point the crests of the material wave are capable of overtaking the troughs of the wave before the disappearance of the phonon. Even at a 30-ns phonon lifetime, the one-dimensional model shows the presence of higher harmonics in the grating.

## REFERENCES

1. N. Bloembergen, *Nonlinear Optics* (Benjamin, New York, 1965).
2. N. Bloembergen, "The stimulated Raman effect," Am. J. Phys. **35,** 989–1023 (1967).
3. C. S. Wang, "Theory of stimulated Raman scattering," Phys. Rev. **182,** 482–494 (1969).
4. P. H. Hu, J. A. Goldstone, and S. S. Ma, "Theoretical study of phase conjugation in stimulated Brillouin scattering," J. Opt. Soc. Am. B **6,** 1813–1822 (1989).
5. H. A. Haus and P. Penfield, Jr., "Basic equations and conservation theorems in the electrostriction phonon maser," J. Appl. Phys. **36,** 3735–3739 (1965).
6. S. Hüller, "Stimulated Brillouin scattering off nonlinear ion acoustic waves," Phys. Fluids B **3,** 3317–3330 (1991).
7. B. S. Masson, "Nonlinear evolution of a stimulated Brillouin scattering dynamic grating in a fluid," J. Opt. Soc. Am. B **8,** 378–383 (1991).
8. V. P. Kuznetsov, "Equations of nonlinear acoustics," Sov. Phys. Acoust. **16,** 467–470 (1971).
9. T. Tamir and H. C. Wang, "Scattering of electromagnetic waves by a sinusoidally stratified half-space I. Formal solution and analytic approximations," Can. J. Phys. **44,** 2073–2094 (1966).
10. T. Tamir, "Scattering of electromagnetic waves by a sinusoidally stratified half-space II. Diffraction aspects at the Rayleigh and Bragg wavelengths," Can. J. Phys. **44,** 2461–2494 (1966).
11. S. T. Peng and E. S. Cassedy, "Scattering of light waves at boundaries to parametrically modulated media," in *Proceedings of the Symposium on Modern Optics*, Vol. 17 of MRI Series (Polytechnic, Brooklyn, N.Y., 1967), pp. 299–342.
12. D. Gottlieb and S. A. Orszag, *Numerical Analysis of Spectral Methods: Theory and Application*, CMBS-NSF Regional Conference Series (Society of Industrial and Applied Mathematics, Philadelphia, Pa., 1989).
13. J. Kervorkian and J. D. Cole, *Perturbation Methods in Applied Mathematics*, Vol. 34 of Applied Mathematical Sciences (Springer-Verlag, New York, 1980), p. 152.
14. J. Serrin, "Mathematical principles of classical fluid mechanics," in *Handbuch der Physik*, S. Flügge, ed. (Springer-Verlag, Berlin, 1959), Vol. VIII/I, p. 237.
15. C. Foias, M. S. Jolly, I. G. Kevrekidis, G. R. Sell, and E. S. Titi, "On the computation of inertial manifolds," Phys. Lett. A **131,** 433–436 (1988).